

TECHNICAL REPORT STANDARD PAGE

1. Report No. FHWA/LA.09/457		2. Government Accession No.	3. Recipient's Catalog No.
4. Title and Subtitle The Rideability of a Deflected Bridge Approach Slab		5. Report Date November 2009	
		6. Performing Organization Code	
7. Author(s) Mark Martinez, P.E.		8. Performing Organization Report No. LTRC Project No: 02-2GT State Project No: 736-99-0996	
9. Performing Organization Name and Address Louisiana Transportation Research Center 4101 Gourrier Avenue Baton Rouge, LA 70808		10. Work Unit No.	
		11. Contract or Grant No.	
12. Sponsoring Agency Name and Address		13. Type of Report and Period Covered Final Report (2002-2009)	
		14. Sponsoring Agency Code	
15. Supplementary Notes Conducted in Cooperation with the U.S. Department of Transportation, Federal Highway Administration			
16. Abstract <p>This report presents the findings associated with the development of a new pavement roughness index called the Posted Speed Localized Roughness Index (LRI_{PS}) that can be used to rate the ride quality on bridge approach slabs. Currently established pavement roughness indices, such as ride number (RN), profile index (PI) and international roughness index (IRI) cannot effectively rate approach slabs due to inherent limitations. This study was initiated in support of a Louisiana Quality Initiative (LQI) research effort entitled "Preservation of Bridge Approach Rideability," which sought to investigate methods of improving ride quality on bridge approach slabs [18]. The LRI_{PS} is derived using the accelerometer outputs which high-speed profilers provide. Based on the data collected through this research, vehicle travel can be considered comfortable if the LRI_{PS} is smaller than 1.2; uncomfortable if it is between 1.2 and 6.0; tolerable if between 6.0 and 30; intolerable if between 30 and 150 and unsafe if greater than 150.</p>			
17. Key Words Bridge Bump, Joint Fault, Ride Quality, LRI, LRI _{PS} , RN, IRI, Roughness, Inertia, Index		18. Distribution Statement Unrestricted. This document is available through the National Technical Information Service, Springfield, VA 21161.	
19. Security Classif. (of this report) N/A	20. Security Classif. (of this page) N/A	21. No. of Pages 60	22. Price N/A

Project Review Committee

Each research project has an advisory committee appointed by the LTRC Director. The Project Review Committee (PRC) is responsible for assisting the LTRC Administrator or Manager in the development of acceptable research problem statements, requests for proposals, review of research proposals, oversight of approved research projects, and implementation of findings.

LTRC appreciates the dedication of the following Project Review Committee members in guiding this research study to fruition.

LTRC Administrator

Zhongjie “Doc” Zhang, Ph.D., P.E.

Members

Phil Arena

Jason Chapman

Mark Chenevert

Said Ismail

Jeff Lambert

Masood Rasoulian

Robert Wegener

Directorate Implementation Sponsor

William Temple

Chief Engineer, LADOTD

The Rideability of a Deflected Bridge Approach Slab

by

Mark Martinez, P. E.

Louisiana Transportation Research Center
4101 Gourrier Avenue
Baton Rouge, LA 70808

LTRC Project No. 02-2GT
State Project No. 736-99-0996

conducted for

Louisiana Department of Transportation and Development
Louisiana Transportation Research Center

The contents of this report reflect the views of the author/principal investigator who is responsible for the facts and the accuracy of the data presented herein. The contents do not necessarily reflect the views or policies of the Louisiana Department of Transportation and Development, the Louisiana Transportation Research Center, or the Federal Highway Administration. This report does not constitute a standard, specification, or regulation.

November 2009

ABSTRACT

This report presents the findings associated with the development of a new pavement roughness index called the posted speed localized roughness index (LRI_{PS}) that can be used to rate the ride quality on bridge approach slabs. Currently established pavement roughness indices, such as ride number (RN), profile index (PI), and International Roughness Index (IRI) cannot effectively rate approach slabs due to inherent limitations. This study was initiated in support of a Louisiana Quality Initiative (LQI) research effort entitled “Preservation of Bridge Approach Rideability” that sought to investigate methods of improving ride quality on bridge approach slabs [18]. The LRI_{PS} is derived using the accelerometer outputs that high-speed profilers provide. Based on the data collected through this research, vehicle travel can be considered comfortable if the LRI_{PS} is smaller than 1.2, uncomfortable if it is between 1.2 and 6.0, tolerable if between 6.0 and 30, intolerable if between 30 and 150, and unsafe if greater than 150.

ACKNOWLEDGMENTS

This research was underwritten by the Louisiana Department of Transportation and Development (LADOTD) and was carried out by its research division at the Louisiana Transportation Research Center (LTRC). The author would like to thank his colleagues at LTRC's Pavement Research Group, which includes Zhongjie Zhang, Gary Keel, Mitchell Terrell, Glen Gore, and Shawn Elisar, whose service helped make this research possible.

IMPLEMENTATION STATEMENT

The LRI_{PS} indexing system should be used as a supplement to traditional roughness indexing systems (IRI and RN). IRI and RN should continue to be used to rate steady-state roughness (roads) as the LRI_{PS} is intended only for use in rating localized roughness (bridge approach slabs). A program for retrofitting departmental profilers with the prototype equipment discussed in this study should be undertaken to allow for a comprehensive evaluation of the LRI_{PS} indexing system. It is critical that a variety of profilers (varied suspension systems) be used in this effort to ensure that proper field testing and prototype refinement can be achieved. A comprehensive statewide evaluation of the LRI_{PS} system should also be undertaken to refine the system and to ascertain the condition of Louisiana's bridge inventory.

This is necessary because there is currently no method available that can accurately rate localized roughness and thereby assess the condition of the Department's bridge approach inventory as it relates to such distresses. It has been observed that Louisiana's highway structures have often achieved high states of localized distress before they have come to the attention of pavement management. The LRI_{PS} indexing system, it is expected, will provide a window onto the mechanism of such failure and, thereby, help formulate design and rehabilitation strategies that can minimize the effect.

TABLE OF CONTENTS

ABSTRACT.....	iii
ACKNOWLEDGMENTS	v
IMPLEMENTATION STATEMENT	vii
TABLE OF CONTENTS.....	ix
LIST OF TABLES	xi
LIST OF FIGURES	xiii
INTRODUCTION	1
Problem Statement.....	1
Literature Review.....	1
Response Based Indexing	2
Profile Based Indexing.....	2
Limitations of Profile Based Indexing.....	3
Available Technologies	6
OBJECTIVE	11
SCOPE	13
METHODOLOGY	15
Research Methods.....	15
The Bridge Transition Problem	15
DISCUSSION OF RESULTS	17
Transportability and Suspension Degradation Issues	17
Development of the LRI	24
Development of the LRIPs	28
Profiler Design Issues	29
District Level Survey	30
CONCLUSIONS.....	37
RECOMMENDATIONS.....	39
ACRONYMS, ABBREVIATIONS, AND SYMBOLS	41
BIBLIOGRAPHY.....	43

LIST OF TABLES

Table 1 Preliminary LRI test findings	28
Table 2 Summary of bridges tested	31
Table 3 Summary of LRI testing	33
Table 4 LRI _{PS} scores	35
Table 5 LRI _{PS} indexing system.....	36
Table 6 Regression-based LRI _{PS} versus single-speed LRI _{PS}	36

LIST OF FIGURES

Figure 1	Illustration of difference between time and frequency domains	5
Figure 2	Example of laser and accelerometer outputs and their frequencies	6
Figure 3	High-speed inertial profilometer	7
Figure 4	Influence diagram of pavement riding quality	9
Figure 5	Influence diagrams for smooth and rough pavement surfaces	9
Figure 6	Quarter-car model and related motion equations	17
Figure 7	Space state block diagram of the FVTF	18
Figure 8	Space state block diagram of the RVTF.....	19
Figure 9	Development of the space state block diagram for the TVTF.....	20
Figure 10	Circuit realization of the TVTF.....	23
Figure 11	Circuit realization of an accelerometer based TVTF	25
Figure 12	Bridge approach slabs.....	26
Figure 13	Typical LRI plot for a bridge (test run at 60 mph).....	27
Figure 14	Exponential regression of LRI scores.....	29
Figure 15	Map of bridges tested	32
Figure 16	Exponential regression of LRI scores.....	34
Figure 17	Plot of LRI_{PS} and IRI scores.....	35

INTRODUCTION

Problem Statement

LADOTD initiated the LQI entitled “Preservation of Bridge Approach Rideability” to explore different potential methods of solving what has been observed as an approach-slab settlement problem at bridge ends [18]. The first task of this LQI was to establish a correlation between bridge approach slab rideability and approach slab deformation. An index that can be used to quantify localized concrete slab sag is required for proper indexing of ride quality on bridge transitions where physical slab deformations are known to occur. Traditional methods of roughness indexing (like IRI and RN) along with alternative methods of indexing can provide insights into how localized (non-steady state) distresses which occur at bridge transitions might best be indexed. This report presents findings that resulted from attempts by the LTRC to examine these issues and recommendations as to how localized roughness indexing of bridge ends might best be accomplished.

Literature Review

Specification requirements for ride quality have become a common feature in modern pavement design programs. Contemporary regulatory specifications rely heavily on road-profile indexing algorithms designed to constrain construction practices so smoother roads can be built. Examples of indexing algorithms that have been used include the RN, PI, and IRI [8], [9], [14]. Each algorithm in its own manner, with distinct advantages and disadvantages, is able to quantify a pavement’s steady-state ride quality [15], [17].

There has been much debate as to how roughness indexing should be developed and employed [17], [16]. In principle, ride quality assessment is a function of the interaction between a vehicle suspension system and the road profile it encounters. This interaction, termed vehicular response, is the basis of all modern ride quality indexing systems. Few make references to it directly. PI and IRI, for example, are calculated exclusively from road profile data and, thus, make no direct reference to vehicular response as part of their development. The means by which PI and IRI are linked to vehicular response (and, therefore, also to ride quality) is by way of reference to a globally developed model called the Golden-Quarter-Car

[5]. The development of this model and the ramifications of its use must be understood if currently used indexing methods are to be properly implemented and if unique problems associated with bridge-bump indexing are to be properly appreciated.

Response Based Indexing

The simplest way to evaluate a road's roughness is to let a passenger rate the ride subjectively by the "seat of his pants." The earliest road roughness measurement systems evaluated ride quality using approaches that exploited this fact. Such systems are referred to as response-type road roughness measuring systems (RTRRMS). The Mays Ride Meter is, by far, the most common RTRRMS currently in use. Such devices determine the smoothness of a roadway by measuring the relative motion of the vehicle's spring mass in response to traveled surface where the mass is supported by the automobile's suspension and tires. The method is very similar to the approach used in seismography. The more dynamic the vehicular motion, the greater the ride index will be.

Although RTRRMS can easily index ride quality very accurately, they are known to have several negative effects. Typically, the dynamics of the host vehicle will not remain stable over time (suspension degradation). Measurements made today with road meters cannot be compared with confidence to those made from the same meter several years ago. Also, RTRRMS smoothness measurements are not transportable (system uniqueness), which means that road meter measurements made by one system are seldom reproducible by another. For example, a heavy profiler that employs tight suspension will yield a very different ride from a lighter profiler employing loose suspension.

Profile Based Indexing

These problems led researchers to propose a ride indexing system that allowed ride quality to be assessed using only a road's profile. Such an approach meant that ride quality could be determined without the need for test equipment to actually "ride" roads in order to monitor and collect vehicular response. Because there was no need to collect vehicular response, the data collection process did not have to proceed at posted speed limits. A road profile could, technically, be collected by rod-and-level survey. But, because this was impractical, devices

like the Australian Road Research Board (ARRB) walking profiler were developed to meet the requirements.

Ride quality was assessed through the development of a quarter-car model that could be made to mathematically “drive” over the collected profile thereby allowing for the assessment of vehicular response. Two National Cooperative Highway Research Program (NCHRP) studies provided for the establishment of this model that is termed the Golden-Quarter-Car [8], [9]. Once the model was developed, various studies examined what components of the road profile impacted ride quality most. This led to the development of filter algorithms designed to accentuate the worst components, and indexing systems were proposed. This is how index algorithms like RN and International Roughness Index (IRI) were established. Once the Golden-Quarter-Car concept took hold, efforts aimed at directly applying vehicular inertia were widely abandoned and most research turned toward trying to either refine the correlation models or directed toward improving the means of recording profiles [14], [2], [1], [6], [7], [12].

Limitations of Profile Based Indexing

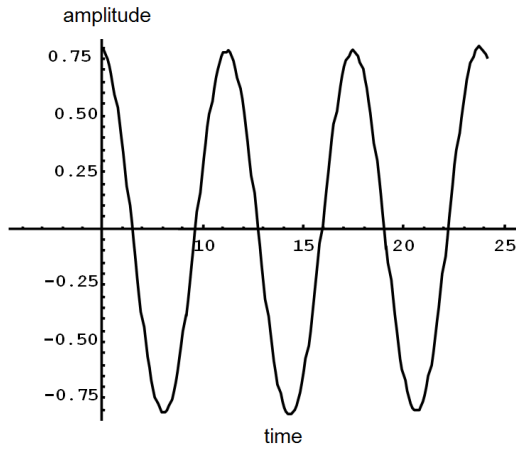
The parameters of IRI and RN algorithms, which employ filtering in the frequency domain, make use of classical time series modeling [14], [13]. A fundamental assumption associated with time series modeling when carried into the frequency domain is that the value of a reading in a series of collected elevations, x_t , at time t depends on its previous values (a deterministic quantity) and on a continuing and predictable random disturbance (a stochastic quantity). It requires that at any given point along a profile, future randomness is statistically similar to past randomness. This means that indexes like RN and IRI are not calculated on a point but are calculated on a window of points similar to the way in which a moving average operates on a window as well. This window, for the IRI, is on the order of 91.4 m (300 ft.) because this is the effective length of road that can impart inertial effects onto a typical moving vehicle.

Profile based roughness estimation methods assess ride quality by way of frequency domain filtering. For example, IRI estimates are derived as a steady-state and broad-bandwidth

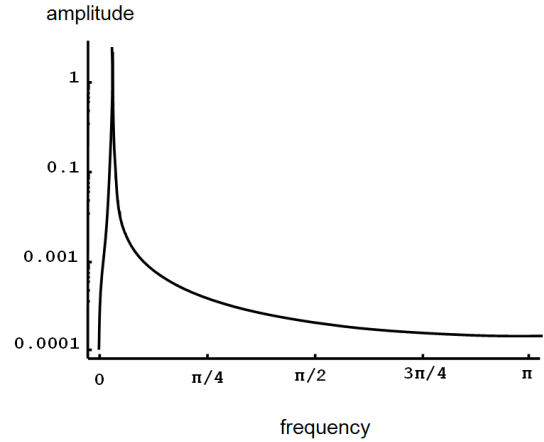
calculation that isolates wavelength components of pavement surfaces within a certain frequency range. Frequencies with wavelengths between 1.2 m (3.9 ft.) and 30 m (98.4 ft.) have optimal impact [16]. Profile conditions on a road that manifest themselves as long sweeping curves are filtered out by the IRI algorithm as are those features of micro-texture that are so short they can be considered inconsequential because the tires of the vehicle span them [14], [12]. Essentially, an IRI score is an estimate of the roughness on a 91.4 m (300 ft.) segment of road (approximate) based on the presence of a unique distribution of component sinusoids that have wavelengths in the 1.2 to 30 m (3.9 to 98.4 ft.) range.

One reason that profile based indexing techniques should not be used to evaluate localized roughness derives from the fact that profiles associated with localized phenomena are generally less than 1.2 m (3.9 ft.) in length and, therefore, outside the target IRI range. But, more importantly, profiles associated with localized phenomena are non-steady-state (i.e., they are both impulsive and non-oscillatory). Non-steady-state phenomena are much harder to deal with in the frequency domain than are steady-state recursive phenomena. Frequency domain analysis methods are designed to analyze recursive patterns where filtering techniques can be used to easily quantify and isolate recursive patterns. This is much harder to do for short, non-oscillatory response phenomena such as are produced by bridge bumps, see Figure 1.

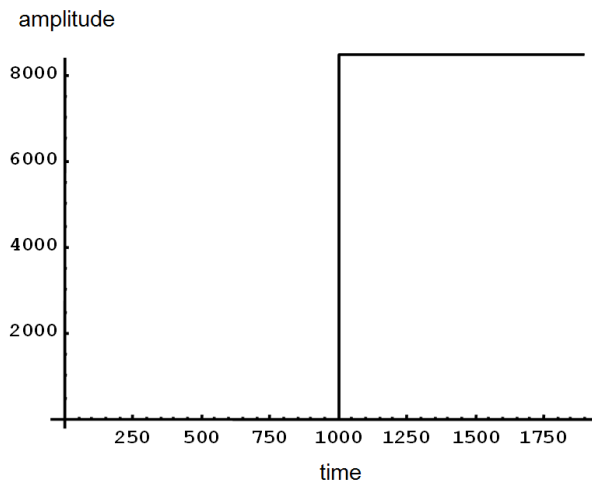
The steady-state sinusoidal profile shown in Figure 1a appears in the frequency domain as a very simple spike in Figure 1b. By contrast, the non-steady-state step function shown in Figure 1c appears in the frequency domain as a very complicated and distributed waveform in Figure 1d. IRI filtering in the frequency domain will properly index the sinusoid. It will, however, not properly index the step function.



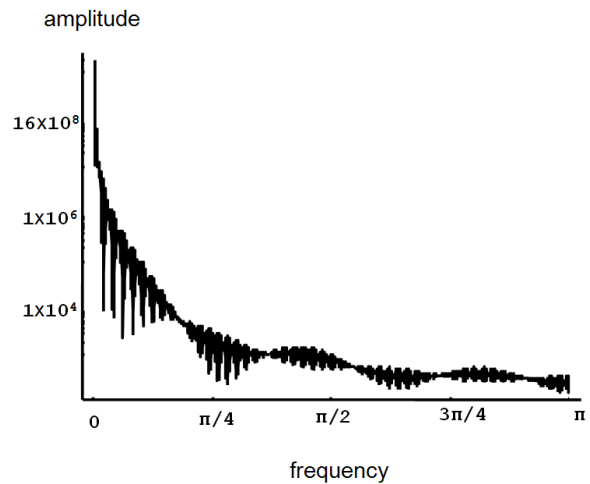
a. Sinusoidal curve in time domain



b. Sinusoidal curve in frequency domain



c. Step function in time domain

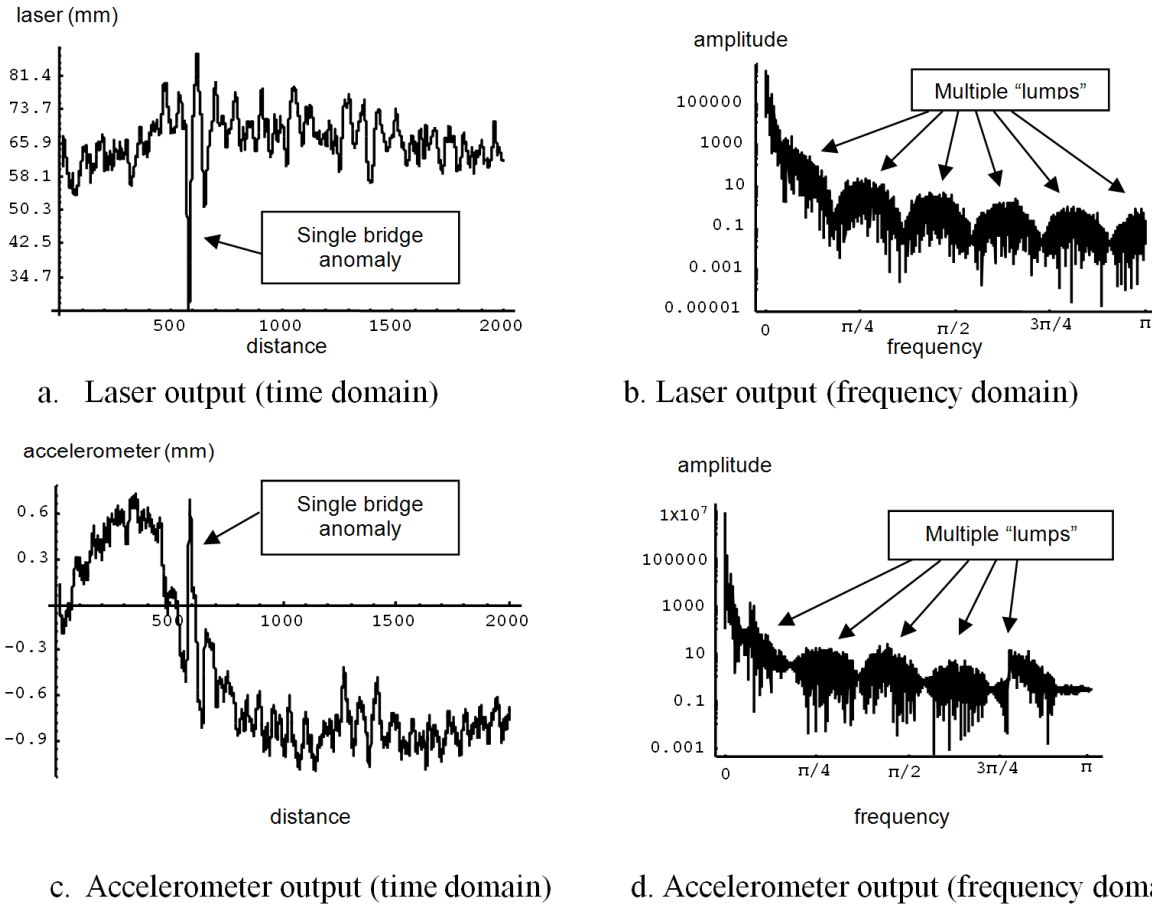


d. Step function in frequency domain

Figure 1
Illustration of difference between time and frequency domains

Figure 2 is provided so the problem can be examined with respect to bridge bumps. Figures 2a and 2c typify the sensor outputs produced by a high-speed laser profiler as it travels over a bridge bump. Figures 2b and 2d show the curves transferred into the frequency domain. What is to be discerned from these plots is that the bridge bump stands out very clearly in both of the time domain plots as an isolated event near the x-axis value of 600. This ease of identification suggests it would be reasonably easy to index the bridge bump in the time domain. By contrast, in the spectral plots, the effect of the bump is reflected continuously, discernable only as a series of lump-like forms that repeat over the length of the plots. This

recursion in the frequency domain makes identifying and indexing the bridge bump comparatively difficult.



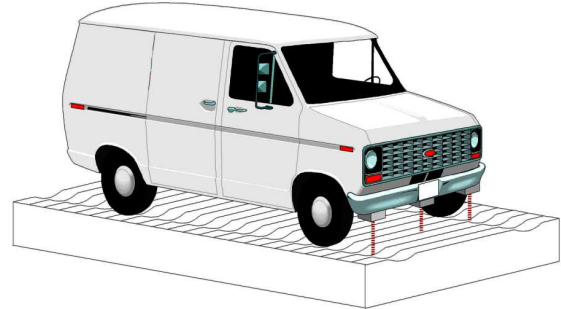
Note: The laser plots in Figure 2 (a and b) are based on bumper elevation (not road profile). As bumper elevation approximates profile, it is considered sufficient to illustrate the concepts discussed in the text.

Figure 2
Example of laser and accelerometer outputs and their frequencies

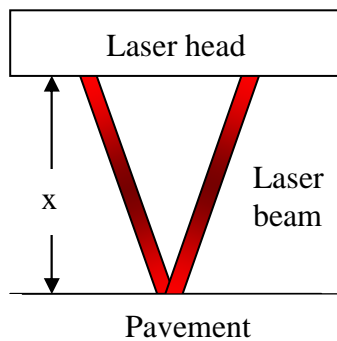
Available Technologies

The high-speed inertial profilometer, see example in Figure 3, makes it possible to measure and record theoretical road surface profiles at speeds between 16 and 112 kph (10 and 70 mph). They are able to generate a pavement’s effective profile through the creation of an inertial reference by using accelerometers placed on the body of the measuring vehicle. Relative displacement between the accelerometer and pavement surface is measured with a

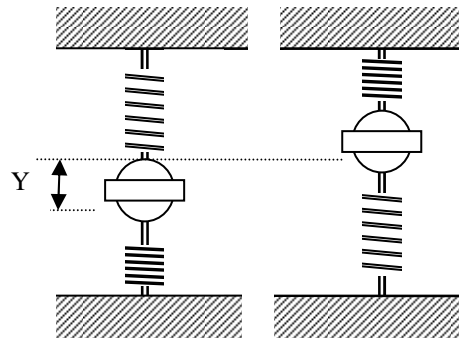
non-contact laser or acoustic measuring device that is mounted alongside the accelerometer on the vehicle body [4]. Devices in this category of equipment include the Kenneth J. Law (K.J. Law) profilometer, the South Dakota profiling device, and the International Cybernetics Corporation (ICC) surface profiling system.



a. Mini-van with laser and inertial sensors



b. Diagram of laser sensor



c. Diagram of inertial sensor

Figure 3
High-speed inertial profilometer

The advantage of these devices is that they allow for a coordinated collection of instantaneous vehicular elevation data and vehicular inertia data at typical highway speeds. On-board software allows these devices to arrive at a pavement's theoretical profile by back-calculation from its ride characteristics as recorded by the system lasers and accelerometers. This distinguishes high-speed profilers from other profile indexing devices (e.g., ARRB Walking Profiler), that arrive at profile by direct measurements in a rod-and-level type fashion. High-speed profilers should be regarded as RTRRMS devices akin to the Mays Ride Meter that rate ride inertially. The principal difference is that high-speed profilers utilize sophisticated

algorithms to convert their ride characteristics, as recorded by a laser and accelerometer, into effective profile.

Evidence that a high-speed laser profiler is an RTRRMS device can be readily seen when its sensor outputs are plotted against each other. An example, termed an influence diagram, is provided in Figure 4. The plot in Figure 4 illustrates the interaction that will typically develop between a profiler's laser and accelerometer signals as the profiler approaches and passes over a bridge bump. The plot records the profiler's accelerometer output in mm along the x-axis and its laser output in mm along the y-axis. The reason the accelerometer units in Figure 4 are given in terms of mm instead of the expected mm/s^2 is because profilers generally process their accelerometer signals through an on-board, second-order integrator algorithm.

The trace in Figure 4 is typical of the moment-by-moment interaction that will form between bumper elevation and inertial response as a bridge bump is approached and passed over by a profiler. Most of the trace that appears in the plot represents the steady-state condition the IRI algorithm was designed for. The dense cluster located around the laser reading of 70 mm and the accelerometer reading of -0.75 mm is a manifestation of steady-state conditions and represents normal roughness of the road on the approach leading up to the bump. Ride quality is a measure of cluster "fuzziness." The concept can be readily seen in Figure 5. The signal produced by a smooth road, Figure 5a, shows up as a tight cluster. A rough road, Figure 5b, produces a broader, fuzzier cluster. The fuzziness in both plots is purely a function of the road's normal roughness and is **not** a consequence of any localized disturbances, such as a bridge bump.

Localized roughness, by comparison, appears in an influence diagram as deviations from the steady-state clusters. The bridge bump in Figure 4 appears in the plot as broad sweeping elliptical forms that sweep out from the tight cluster previously mentioned. These ellipses record the non-linear response that resulted because of the bridge-bump. The wider and more erratic these elliptical patterns are, the more pronounced is the effect of the bump. Such deviations, indicative of localized roughness are too transitory for profile based indexing to

catch. The localized roughness index (LRI) developed in this research attempts to index such phenomena directly from the profiler's inertial outputs.

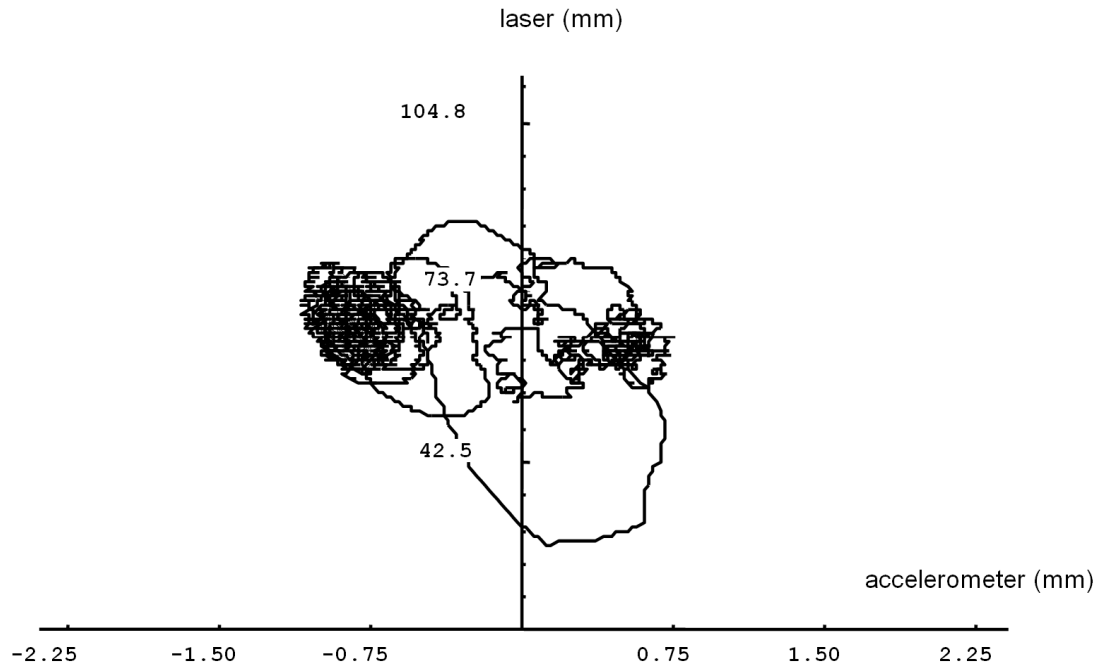


Figure 4
Influence diagram of pavement riding quality

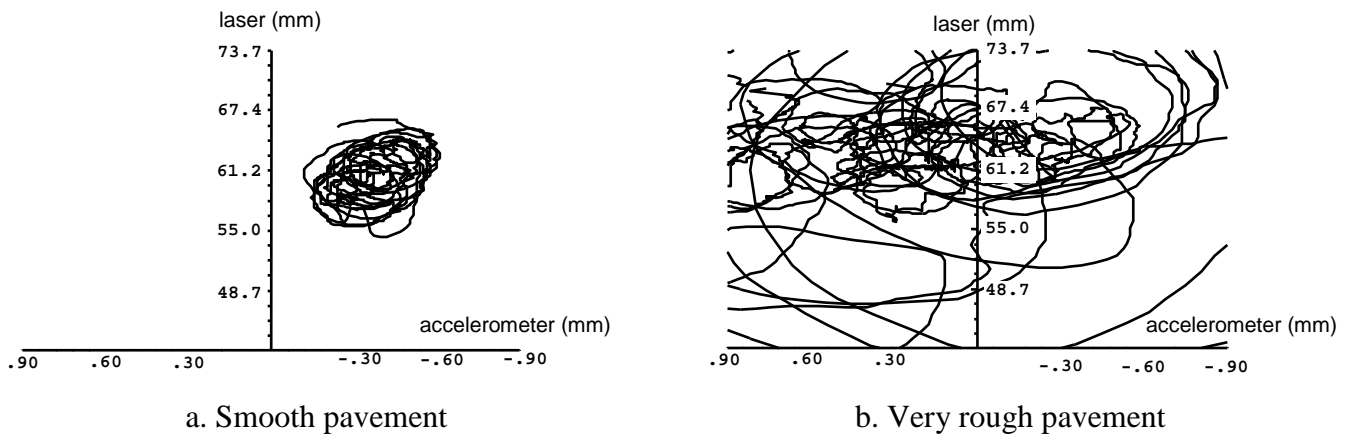


Figure 5
Influence diagrams for smooth and rough pavement surfaces

OBJECTIVE

This research is initiated in response to the requirements of the LQI study entitled “Preservation of Bridge Approach Rideability” whose primary objective is to investigate methods of preserving the ride quality of bridge approach slabs that are technically feasible, designable, constructible, and cost-effective.

In support of the LQI, the primary objective of this sub-study is to examine possible methods of evaluating localized roughness so ride quality associated with impulsive phenomena like bridge bumps can be indexed. This is necessary because current indexing systems like the IRI and RN are known to have problems assessing such phenomena.

A secondary objective of this study is to attempt to carry the research beyond theory by developing a prototype device that will realize this proposed index in an inexpensive and easily implementable manner.

SCOPE

For this research, approximately 12 bridges (3 for a preliminary investigation supplemented by an additional 9 for a district level survey) were analyzed using LADOTD's laser profiling equipment. The first three bridges served as a control group selected to represent the range of ride conditions that could occur in the field with rides ranging from very comfortable to near hazardous. An additional 9 bridges were randomly selected and tested so results could be used to explore what typical ride conditions in Louisiana might be.

METHODOLOGY

Research Methods

The Bridge Transition Problem

Preliminary research efforts began with attempts to use IRI indexing methods to evaluate a number of bridge approaches in the vicinity of Baton Rouge. Evaluation of the collected data showed results were inconclusive. An examination of literature revealed that profile-based indexing, exemplified by IRI, does not work well on short-duration impulsive inertial phenomena, like those found at distressed bridge approaches. For this reason, it was determined that an RTRRMS approach to indexing would be required. Of the various RTRRMS technologies available, it was determined that research would utilize a high-speed laser profiler because it allowed for quick field testing that would have little impact on traffic. Road closures, for example, would not be necessary while tests were being conducted.

Basing the proposed bridge index, LRI, on vehicular response presented a problem because it meant that it would lack transportability (indexing results would vary from vehicle to vehicle because of differences in their suspension systems). Literature showed the transportability problem could be overcome through the development of a transfer function that could translate one vehicle's response into another. Such a transfer function was, therefore, developed and prototyped through the employment of classical circuit realization techniques commonly used in control systems engineering.

It was discovered that the proposed LRI could be effectively expressed in terms of the output of a high-speed laser profiler's accelerometer. It was observed that a laser profiler's accelerometers produced a highly amplified burst of oscillation when it encountered a bridge bump or other such localized phenomena. Taking the squared variance of the accelerometer signal proved sufficient to serve as the basis for the proposed index. The only difficulty associated with taking the squared variance was that the index proved to be impractical. Extremely distressed bumps often produced LRI scores in the millions. To overcome this, all LRI scores were divided by 100,000 to ensure that scores were manageable.

Once an indexing algorithm was developed, LADOTD's inventory of bridges was canvassed to find a number of bridges that could be used to calibrate the LRI. Three bridges were isolated in this capacity. They expressed widely ranging roughness characteristics; the smoothest bridge transition was able to provide a very comfortable ride at all speeds, while the roughest bridge transition was barely passable at higher speeds. These three bridges were run at three different speeds so LRI results for each bridge could be plotted versus speed. The LRI value that corresponded to the bridge's posted speed, a new index termed the LRI_{PS} (Posted Speed Localized Roughness Index), was then interpolated from each plot. These interpolated figures were then used to establish performance ranges.

Once LRI performance ranges had been established, LRI scores from 11 randomly chosen bridges were compiled and analyzed. This was carried out to evaluate the general ride quality of bridge transitions within a given parish in an effort to qualify the meaning of the LRI_{PS} scores. For this survey operation, the bridges were selected from within East Baton Rouge (EBR) parish where LTRC's profiler was stationed. Testing was conducted in the same manner that was carried out in the calibration effort (each bridge was tested at four speeds so the LRI_{PS} could be interpolated from the associated plots). Each test was also panel-rated by a clipboard survey to qualify scores.

A significant operational difficulty presented itself early during the initial calibration effort that impacted the progress of research. Accelerometers and lasers used on high speed-profilers often clip when they experience extreme bounces while traversing a severe bridge-bump or joint fault, especially at high speeds. The LTRC profiler used in the opening phases of this research suffered from this weakness. For this reason, a new prototype profiler was developed that was outfitted with more robust sensors to overcome the problem; it was this rig that was employed to test the 12 bridges described.

DISCUSSION OF RESULTS

Transportability and Suspension Degradation Issues

RTRRMS approaches to roughness indexing require that problems associated with the lack of transportability (ride quality varies between vehicles because of differences in their suspension systems) and suspension degradation (ride quality falsely appears to worsen as a consequence of suspension system aging) be overcome. Literature shows that control theory, an interdisciplinary branch of engineering and mathematics that deals with the behavior of dynamical systems could be used to overcome these problems [11], [10]. This theory allows a physical system's input signal to be mathematically linked to its output signal. In the case of high-speed profilers, it links the profiler's inertial response (output signal) to the road profile that caused it (input signal). Development of a mathematical model of the profiler's suspension system is required to realize the opportunities that control theory affords.

In its simplest form, a profiler's quarter-car suspension can be expressed dynamically by the system shown in Figure 6 where m_s , m_u , c_s , c_u , k_s , k_u , z_0 , z_u , and z_s represent the vehicle mass, tire mass, shock absorber spring constant, tire compression spring constant, shock absorber damping factor, tire compression damping factor, road profile as a function of time, axle elevation as a function of time, and vehicle body elevation as a function of time, respectively. The motion equations, given in Figure 6, model the way in which these factors interact with each other dynamically as a profiler travels down the road.

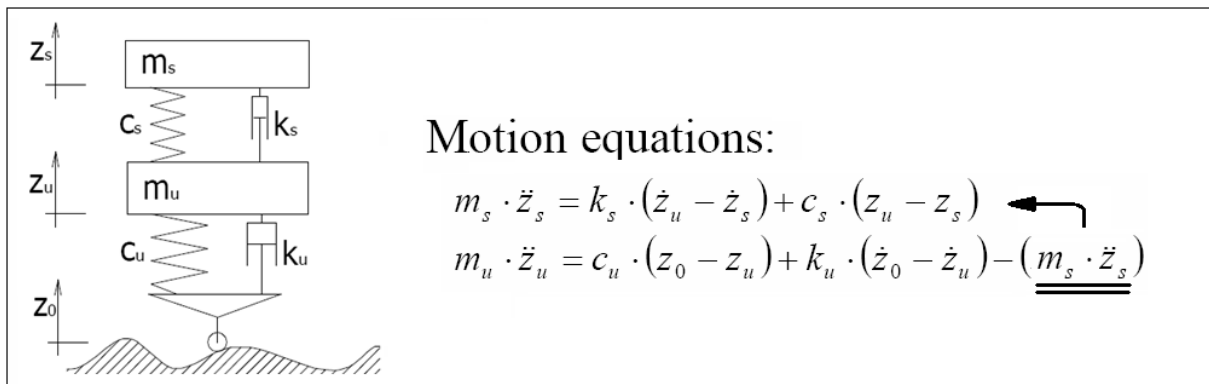


Figure 6
Quarter-car model and related motion equations

\mathcal{L} -Transformation techniques can be used to derive a transfer function that relates road profile (z_0) to vehicular response (z_s) [3]. This relationship is given by the following equation:

$$\frac{Z_s}{Z_0} = \frac{b_4 \cdot s^2 + b_1 \cdot s + b_0}{a_4 \cdot s^4 + a_3 \cdot s^3 + a_2 \cdot s^2 + a_1 \cdot s + a_0} \quad (1)$$

where,

$$\begin{aligned} a_0 &= \frac{c_u \cdot c_s}{m_u \cdot m_s} & b_0 &= \frac{c_u \cdot c_s}{m_u \cdot m_s} \\ a_1 &= \frac{c_u \cdot k_s}{m_u \cdot m_s} + \frac{c_s \cdot k_u}{m_u \cdot m_s} & b_1 &= \frac{c_u \cdot k_s}{m_u \cdot m_s} + \frac{c_s \cdot k_u}{m_u \cdot m_s} \\ a_2 &= \frac{c_u}{m_u} + \frac{k_u \cdot k_s}{m_u \cdot m_s} + \frac{c_s}{m_u} + \frac{c_s}{m_s} & b_4 &= \frac{k_u \cdot k_s}{m_u \cdot m_s} \\ a_3 &= \frac{k_u}{m_u} + \frac{k_s}{m_s} + \frac{k_s}{m_u} & a_4 &= 1 \end{aligned}$$

Note: The “s” term in equation (1) is an operator associated with Laplace transformation techniques that models differentiation in the time domain. A complete treatment of s-domain analysis can be found in any fundamentals of systems and signals analysis text such as McGillem and Cooper, 1984.

The transfer function allows a high-speed profiler to determine a road’s profile from its inertial reaction. The block diagram in Figure 7 illustrates that if the vehicular response is inputted into a circuit realization of the transfer function, which will be termed the forward vehicular transfer function (FVTF), then the output will be the road profile. This is how high-speed profilers arrive at road profile.

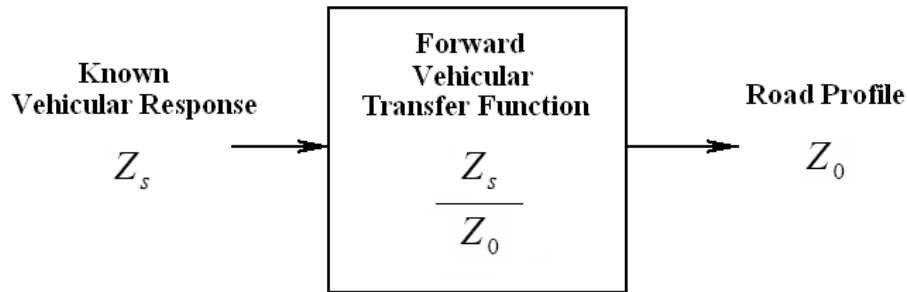


Figure 7
Space state block diagram of the FVTF

It is possible to implement such a transfer function in reverse wherein road profile is used as the input and vehicular response is produced as the output. This might be termed the reverse vehicular transfer function (RVTF) and would resemble the block diagram shown in Figure 8 wherein the defining equation would be as follows (terms defined as above):

$$\frac{Z_0}{Z_s} = \frac{a_4 \cdot s^4 + a_3 \cdot s^3 + a_2 \cdot s^2 + a_1 \cdot s + a_0}{b_4 \cdot s^2 + b_1 \cdot s + b_0} \quad (2)$$

The Golden-Quarter-Car is an example of a RVTF in action. The parameters of the Golden-Quarter-Car were set by committee agreement. These parameters were considered by this committee to be representative of what would be found on a typical passenger car, which they termed the “golden car.” This golden car model accepts road profile (z_o) as its input and produces the golden car’s vehicular response (z_s) on output. It should be noted that profile based indexing methods like IRI fail to index phenomena like bridge bumps not because the transfer function models are inadequate. Rather, they fail because they attempt to isolate the profile characteristics that will cause the most severe reaction of the golden car through the employment of Fourier analysis techniques. Such techniques involve expressing profiles in the frequency domain and, as has been explained, bridge bumps cannot be expressed in the frequency domain well.

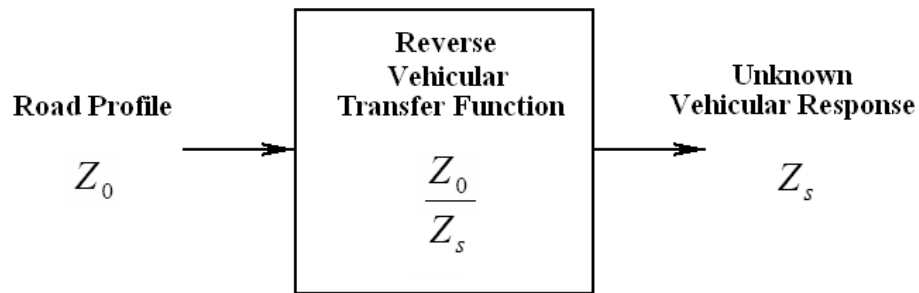
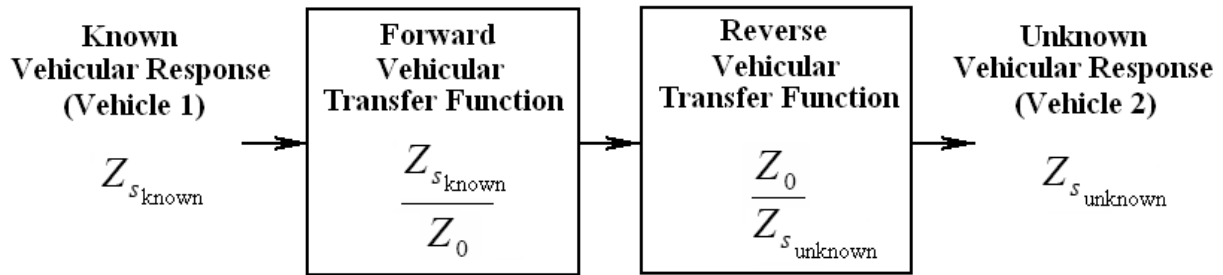


Figure 8
Space state block diagram of the RVTF

Linking the block diagrams in Figures 7 and 8 in a series provides a means of overcoming the transportability and suspension degradation problems discussed. Figure 7 shows that it is possible to determine a road profile from a vehicles response. Figure 8 shows that it is possible to determine a vehicle’s response from a road profile. If it is assumed that the road profile is the same in both figures, then it is possible to determine the response of one vehicle

to that profile by examining the response of the other. The model that realizes this is given in Figure 9. The transfer function produced by combining the FVTF of the vehicle whose response is known to the RTVF of the vehicle that is unknown can be termed the translational vehicular transfer function (TVTF). The defining equation for the TVTF is as follows:

$$\frac{Z_{s_{unknown}}}{Z_{s_{known}}} = \frac{(b_4 \cdot s^2 + b_1 \cdot s + b_0)_{unknown} \cdot (a_4 \cdot s^4 + a_3 \cdot s^3 + a_2 \cdot s^2 + a_1 \cdot s + a_0)_{known}}{(a_4 \cdot s^4 + a_3 \cdot s^3 + a_2 \cdot s^2 + a_1 \cdot s + a_0)_{unknown} \cdot (b_4 \cdot s^2 + b_1 \cdot s + b_0)_{known}} \quad (3)$$



Which can be expressed as:

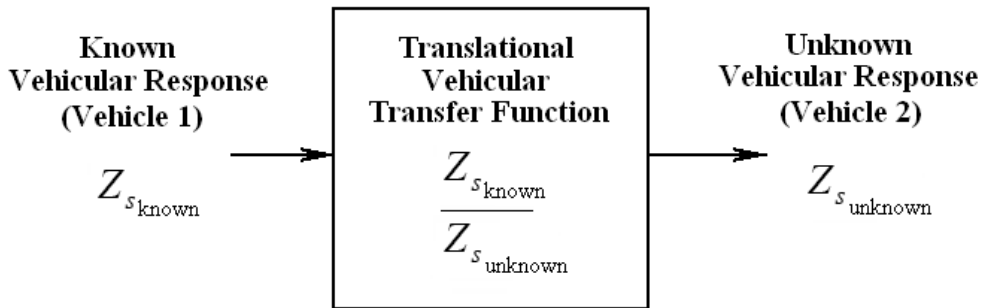


Figure 9
Development of the space state block diagram for the TVTF

It is possible to develop a circuit realization of the TVTF by simplifying its equation. Using Ferrari's Method for finding the roots of quartic functions it is possible to express the TFTV equation as follows (the u and k subscripts stand for unknown and known, respectively):

$$\frac{Z_{s_u}}{Z_{s_k}} = \frac{(s - A_{1k})(s - A_{2k})(s - A_{3k})(s - A_{4k})(s - B_{1u})(s - B_{2u})}{(s - B_{1k})(s - B_{2k})(s - A_{1u})(s - A_{2u})(s - B_{3u})(s - B_{4u})} \quad (4)$$

where,

$$B_{1u} = \frac{-b_{1u} - \sqrt{b_{1u}^2 - 4 \cdot b_{4u} \cdot b_{0u}}}{2 \cdot b_{4u}}$$

$$B_{2u} = \frac{-b_{1u} + \sqrt{b_{1u}^2 - 4 \cdot b_{4u} \cdot b_{0u}}}{2 \cdot b_{4u}}$$

$$\alpha_u = \frac{3 \cdot a_{3u}^2}{8 \cdot a_{4u}^2} + \frac{a_{2u}}{a_{4u}}$$

$$\beta_u = \frac{a_{3u}^3}{8 \cdot a_{4u}^3} - \frac{a_{3u} \cdot a_{2u}}{2 \cdot a_{4u}^2} + \frac{a_{1u}}{a_{4u}}$$

$$\gamma_u = -\frac{3 \cdot a_{3u}^4}{256 \cdot a_{4u}^4} + \frac{a_{2u} \cdot a_{3u}^2}{16 \cdot a_{4u}^3} - \frac{a_{3u} \cdot a_{1u}}{4 \cdot a_{4u}^2} + \frac{a_{0u}}{a_{4u}}$$

$$A_{1u} = -\frac{a_{3u}}{4 a_{4u}} + \frac{W_u + \sqrt{-(3\alpha_u + 2Y_u + \frac{2\beta_u}{W_u})}}{2}$$

$$A_{2u} = -\frac{a_{3u}}{4 a_{4u}} + \frac{W_u - \sqrt{-(3\alpha_u + 2Y_u + \frac{2\beta_u}{W_u})}}{2}$$

$$A_{3u} = -\frac{a_{3u}}{4 a_{4u}} + \frac{-W_u + \sqrt{-(3\alpha_u + 2Y_u - \frac{2\beta_u}{W_u})}}{2}$$

$$A_{4u} = -\frac{a_{3u}}{4 a_{4u}} + \frac{-W_u - \sqrt{-(3\alpha_u + 2Y_u - \frac{2\beta_u}{W_u})}}{2}$$

$$P_u = -\frac{\alpha_u^2}{12} - \gamma_u \quad Q_u = -\frac{\alpha_u^3}{108} + \frac{\alpha_u \cdot \gamma_u}{3} - \frac{\beta_u^2}{8}$$

$$R_u = -\frac{Q_u}{2} \pm \sqrt{\frac{Q_u^2}{4} + \frac{P_u^3}{27}} \quad (\text{use either sign})$$

$$U_u = \sqrt[3]{R_u} \quad W_u = \sqrt{\alpha_u + 2Y_u}$$

$$Y_u = \begin{cases} \text{if } U_u = 0: & -\frac{5\alpha_u}{6} - \sqrt[3]{Q_u} \\ \text{if } U_u \neq 0: & -\frac{5\alpha_u}{6} + U_u - \frac{P_u}{3U_u} \end{cases}$$

Note: Terms in the TFTV equation with a k subscript are found by substituting k for u in all the supporting equations

The TFTV equation can be further simplified by partial fraction decomposition:

$$\frac{Z_{S_u}}{Z_{S_k}} = \frac{N_1}{(D_1 \cdot s + 1)} + \frac{N_2}{(D_2 \cdot s + 1)} + \frac{N_3}{(D_3 \cdot s + 1)} + \frac{N_4}{(D_4 \cdot s + 1)} + \frac{N_5}{(D_5 \cdot s + 1)} + \frac{N_6}{(D_6 \cdot s + 1)} + 1 \quad (5)$$

where,

$$D_1 = \frac{1}{(-B_{1k})} \quad D_2 = \frac{1}{(-B_{2k})} \quad D_3 = \frac{1}{(-A_{1u})} \quad D_4 = \frac{1}{(-A_{2u})} \quad D_5 = \frac{1}{(-A_{3u})} \quad D_6 = \frac{1}{(-A_{4u})}$$

$$N_1 = D_1 \cdot \frac{(B_{1k} - A_{1k})(B_{1k} - A_{2k})(B_{1k} - A_{3k})(B_{1k} - A_{4k})(B_{1k} - B_{1u})(B_{1k} - B_{2u})}{(B_{1k} - B_{2k})(B_{1k} - A_{1u})(B_{1k} - A_{2u})(B_{1k} - B_{3u})(B_{1k} - B_{4u})}$$

$$N_2 = D_2 \cdot \frac{(B_{2k} - A_{1k})(B_{2k} - A_{2k})(B_{2k} - A_{3k})(B_{2k} - A_{4k})(B_{2k} - B_{1u})(B_{2k} - B_{2u})}{(B_{2k} - B_{1k})(B_{2k} - A_{1u})(B_{2k} - A_{2u})(B_{2k} - B_{3u})(B_{2k} - B_{4u})}$$

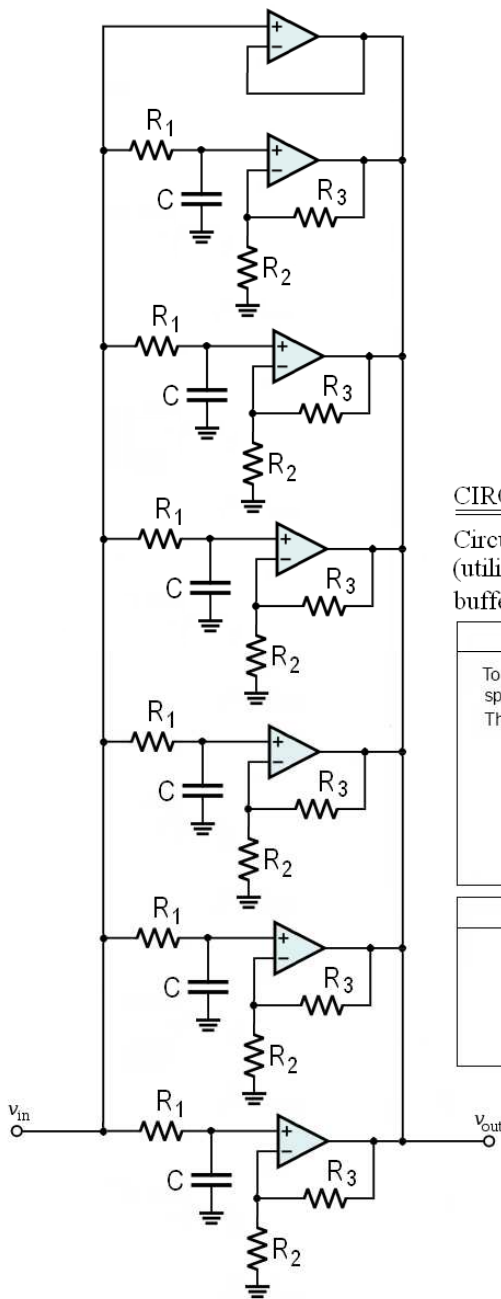
$$N_3 = D_3 \cdot \frac{(A_{1u} - A_{1k})(A_{1u} - A_{2k})(A_{1u} - A_{3k})(A_{1u} - A_{4k})(A_{1u} - B_{1u})(A_{1u} - B_{2u})}{(A_{1u} - B_{1k})(A_{1u} - B_{2k})(A_{1u} - A_{2u})(A_{1u} - B_{3u})(A_{1u} - B_{4u})}$$

$$N_4 = D_4 \cdot \frac{(A_{2u} - A_{1k})(A_{2u} - A_{2k})(A_{2u} - A_{3k})(A_{2u} - A_{4k})(A_{2u} - B_{1u})(A_{2u} - B_{2u})}{(A_{2u} - B_{1k})(A_{2u} - B_{2k})(A_{2u} - A_{1u})(A_{2u} - B_{3u})(A_{2u} - B_{4u})}$$

$$N_5 = D_5 \cdot \frac{(A_{3u} - A_{1k})(A_{3u} - A_{2k})(A_{3u} - A_{3k})(A_{3u} - A_{4k})(A_{3u} - B_{1u})(A_{3u} - B_{2u})}{(A_{3u} - B_{1k})(A_{3u} - B_{2k})(A_{3u} - A_{1u})(A_{3u} - A_{2u})(A_{3u} - B_{4u})}$$

$$N_6 = D_6 \cdot \frac{(A_{4u} - A_{1k})(A_{4u} - A_{2k})(A_{4u} - A_{3k})(A_{4u} - A_{4k})(A_{4u} - B_{1u})(A_{4u} - B_{2u})}{(A_{4u} - B_{1k})(A_{4u} - B_{2k})(A_{4u} - A_{1u})(A_{4u} - A_{2u})(A_{4u} - B_{3u})}$$

Partial fraction decomposition simplifies the TFTV such that circuit realization techniques can be used to develop a prototype device that accomplishes the operation laid out in Figure 9. Each term of the form $N_i/(D_i s + 1)$ can be modeled using a first-order low-pass Op-Amp filter. The unity term shown in the TFTV equation can be modeled using a unity-gain Op-Amp buffer circuit. The summation of terms in the TFTV equation is realized by wiring low-pass filters and buffer stages parallel. A mockup of the overall circuit is provided in Figure 10.



CIRCUIT REALIZATION:

Circuit realization of the TFTV requires six first-order low-pass filter stages (utilizing non-inverting op-amps) to be connected in parallel with a unity-gain buffer stage. The component values for each stage are determined as follows:

First-Order Low-Pass Filter (six stages required)	
<p>To dimension the circuit, specify the capacitor C and the resistor R_3. Then solve for resistors R_1 and R_2:</p> $R_1 = D_i \div C$ $R_2 = R_3(N_i - 1)$	<p>The diagram shows a non-inverting op-amp with a feedback network of resistors R_2 and R_3. The input network consists of a resistor R_1 and a capacitor C connected to the non-inverting input. The input is labeled v_{in} and the output is labeled v_{out}.</p>
Unity-Gain Buffer (one stage required)	
<p>The diagram shows a non-inverting op-amp configured as a unity-gain buffer, with the output connected directly to the non-inverting input. The input is labeled v_{in} and the output is labeled v_{out}.</p>	

Figure 10
Circuit realization of the TVTF

Note that the TVTF circuit in Figure 10 is designed to accept vehicular elevation (actual elevation of the profiler's bumper as a function of time) at v_{in} . This is difficult to determine by field measurement. Vehicular elevation can be pseudo-realized, though, by twice

integrating a profiler's accelerometer signal. Thus, placement of a two-stage integrator circuit at the input of the TVTF circuit allows the prototype to process a profiler's accelerometer signal. Likewise, placement of a two-stage differentiator circuit on the TVTF circuit's output at v_{out} of Figure 10 allows the output of the TVTF to be converted into a prospective profiler's theoretical accelerometer signal.

Combining the two-stage integrator and two-stage differentiator with the TVTF prototype will produce a combinational circuit that accepts a known profiler's accelerometer signal on input and produces a prospective profiler's accelerometer signal on output. The details for this combinational circuit are shown in Figure 11.

Development of the LRI

Initially, attempts were made to develop the LRI through comparative analysis of interdependent field data. This approach required both accelerometer and laser outputs from each field test. This data was plotted as influence diagrams, like the one shown in Figure 5, and analyzed. Although localized roughness could easily be observed in these plots, attempts to develop a working index from them proved to be awkward and the approach had to be abandoned.

Closer examination of data indicated that a comparative analysis of accelerometer and laser signals was not necessary. It was observed that all the effects of localized roughness could be isolated in either of the signals, suggesting it was not necessary to collect both. Figure 2 exemplifies what was universally observed in the trials. Whenever a phenomenon like a bridge bump was encountered during testing, a short duration burst of highly amplified oscillation could be observed in the accelerometer output in the proximity of the bridge bump. It was also observable in the laser output. Analysis of these resulting signals revealed that a good measure of the ride quality associated with bridge bumps could be obtained by taking the squared variance of either signal over the period of amplified oscillation.

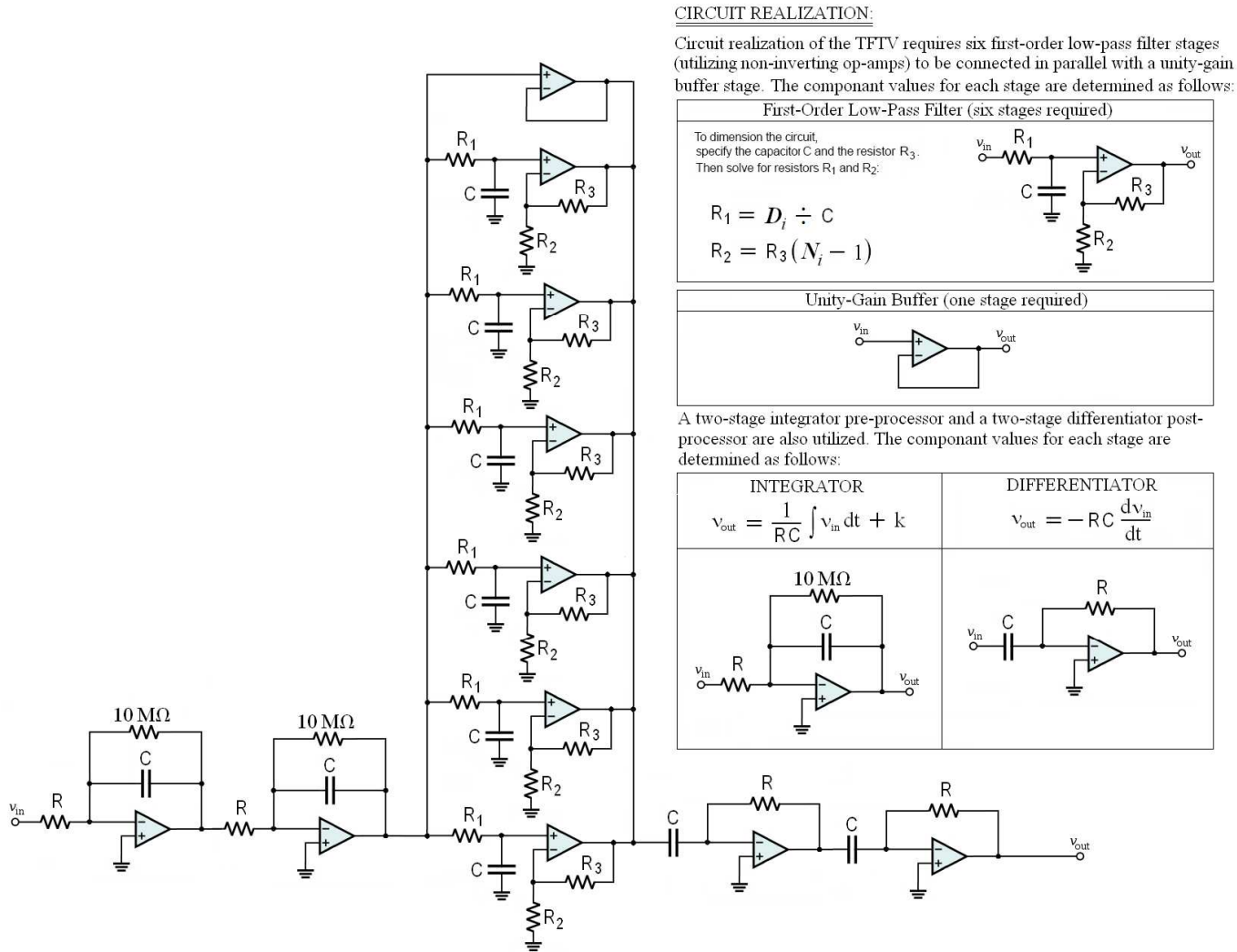


Figure 11
Circuit realization of an accelerometer based TVTF

Although either signal (laser or accelerometer) was considered as a sufficient foundation to build the proposed LRI upon, the decision was made to base it on the accelerometer signal because the prototype circuit developed to overcome the transportability and suspension degradation issues, illustrated in Figure 11, was designed to process accelerometer signals. Doing so would mean no further circuit development would be necessary.

To begin the process of establishing the operational parameters of the LRI, three bridge approach slabs with minor, medium, and severe bumps, as shown in Figure 12, were selected so a wide range of ride conditions could be assessed.



Figure 12
Bridge approach slabs

It was expected that ride quality would vary with speed. To investigate this, the three bridges were profiled at four different speeds. Accelerometer readings were collected at the highest sample rate available (10 readings per foot) so signal resolution could be maximized. To eliminate random noise in the signal, all raw accelerometer data were first filtered using a 6-in. median filter. Once filtered, the LRI for any given point along the pavement was tabulated as the squared variance of accelerometer readings collected within the 1.52 m (5 ft.) of pavement immediately following the point. This 1.52-m (5-ft.) window was selected because it best delineated bridge bumps.

A typical LRI plot for a bridge that was tested at 60 mph is presented in Figure 13. The plot clearly shows a bump with a LRI rating of $551913 \text{ ft}^4/\text{sec}^8$ at the bridge approach located at

about 234.8 m (800 ft.) A less severe bump with a LRI rating of 111,652 ft⁴/sec⁸ is also discernable at the bridge's exit located at about 289.6 m (950 ft.)

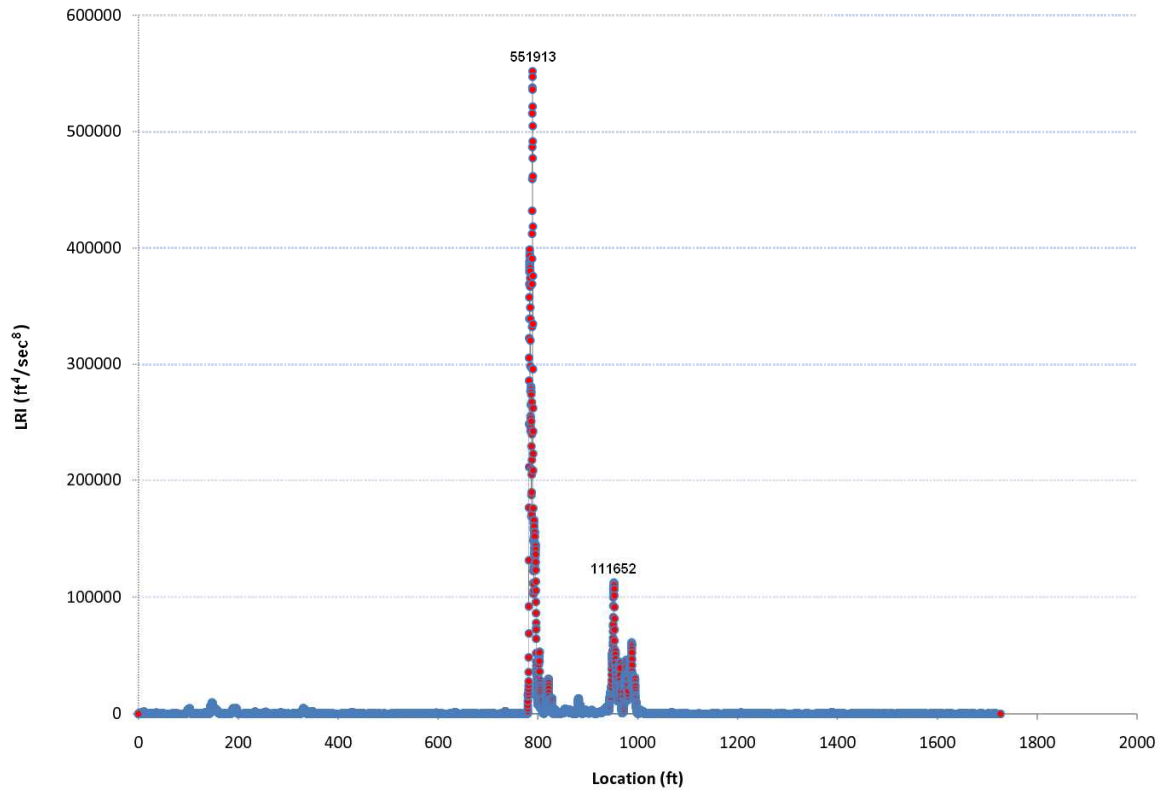


Figure 13
Typical LRI plot for a bridge (test run at 60 mph)

A summary of results from this preliminary testing is presented in Table 1. These findings are plotted and regressed in Figure 14. Figure 14 also illustrates ride quality thresholds as determined by panel rating ranging from comfortable, through uncomfortable, tolerable, intolerable, and unsafe. The rating was developed by a clipboard survey using two to three raters who would score the ride on each bridge approach with a rating of from 1 to 5 (1 being comfortable and 5 being unsafe). The terms uncomfortable, tolerable, and intolerable were chosen arbitrarily to qualify ratings of 2, 3, and 4, respectively.

Table 1
Preliminary LRI test findings

Bridge Bump Severity			
LRI Units, ft⁴/sec⁸			
Speed, (mph)	Minor Bump LA67 (30.6°, -91.1°) (Posted at 55 mph)	Medium Bump US 61 (30.6°, -91.2°) (Posted at 65 mph)	Severe Bump LA 1 (30.5°, -91.2°) (Posted at 55 mph)
60	85324	2322154	15385783
50	56855	1590398	11135218
40	31741	899070	10646764
30	26329	149445	5044707
Exponential	$7058.4e^{0.0411x}$	$15997e^{0.088x}$	$2E+06e^{0.0339x}$
Regression:	$R^2 = 0.9675$	$R^2 = 0.8747$	$R^2 = 0.8608$

Development of the LRI_{PS}

Table 1 indicates that speed greatly impacts LRI ride quality. This was considered a shortcoming because it made interpretation of LRI scores overly complex. Research showed that normalizing LRI results with respect to posted speed limit effectively overcame the problem. LRI normalization methods can be demonstrated through an example: supposing that the posted speed limit for the bridge with the minor bump in Figure 14 were 70 mph, it would be possible to calculate the LRI for this critical speed by plugging 70 into the bridge's regression equation $7058.4e^{0.0411x}$. Doing so produces a projected LRI score equaling 125,364 ft⁴/s⁸, which, according to Figure 14, would be considered uncomfortable. Normalization of LRI scores in this manner effectively overcomes problems cited by yielding an indexing system that operates independently of speed. This normalized index came to be termed the LRI_{PS}.

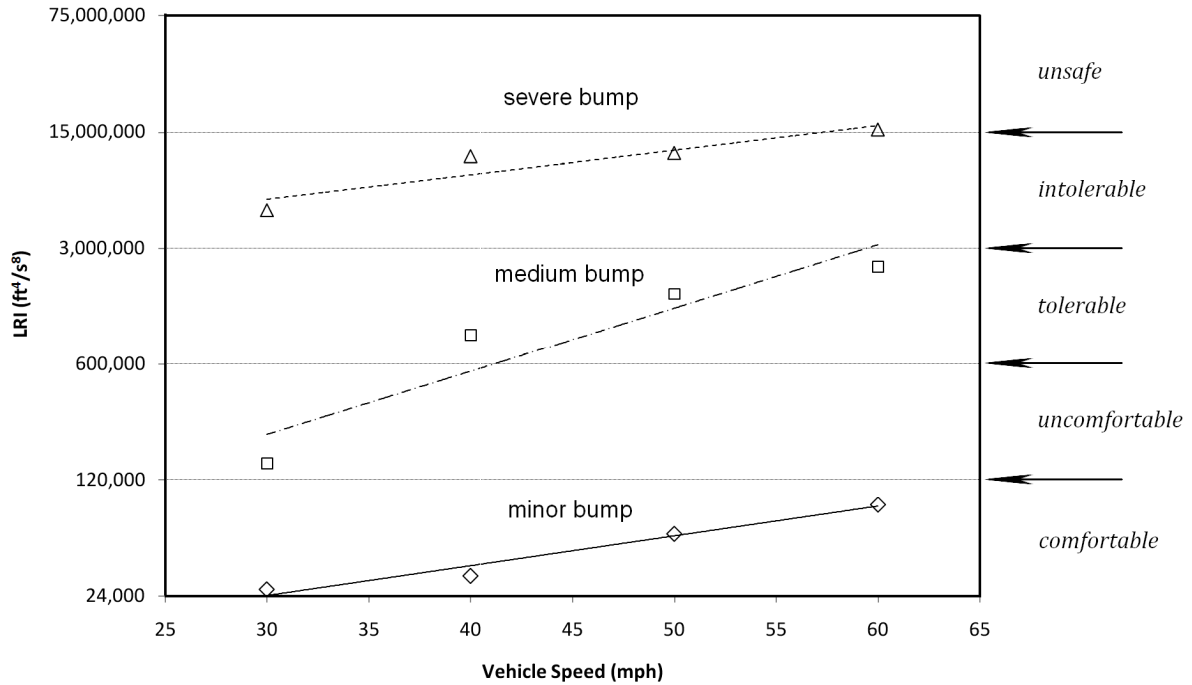


Figure 14
Exponential regression of LRI scores

Profiler Design Issues

The profiler used to develop the findings provided in Table 1 and Figure 14 (as well as for the findings that will be presented in the remainder of this report) was of a modified design. Research attempted to carry out the analysis using the kind of conventional high-speed profiler that would typically be employed to index IRI style road roughness. But, it was quickly determined that a conventional profiler could not drive over severe bumps and joint faults at high speed without its sensors clipping. To overcome this, a prototype profiler was developed on contract that utilized a more robust laser and accelerometer sensor so clipping would not occur. The design integrated prototype and conventional sensors together onto a standard profiler so the rig could be used to conduct conventional profiling as well as bridge profiling.

Design characteristics of this prototype profiler utilized sensors that could collect and output raw data at a rate of 10 samples per foot. This high rate of sampling was required to ensure that signal resolution would be high enough. It was also determined that the system's LRI

sensors (laser and accelerometer) needed to be mounted mid-bumper to minimize the effects of pitch and yaw. Also, it was required that the sensors headroom needed to be large enough to ensure that clipping would not occur.

District Level Survey

The preliminary research carried out on the first three bridges was done to ascertain the maximum and minimum values that the LRI takes on. A follow-up district level survey of randomly selected bridges was conducted to study the functionality of the LRI system and to allow for a comparative analysis to IRI.

For this survey, 11 bridges were randomly selected within the northern part of East Baton Rouge parish in Louisiana's District 61. Note that the LA67 and US61 bridges found in Table 1 were included in this random selection. Table 2 and Figure 15 detail the sites tested. Each bridge was panel-rated and LRI-indexed in the same manner that was used in preliminary testing (panel rating by three raters and quantitative LRI scoring at four speeds). Regression curves like those shown in Figure 14 were developed for each bridge. A tabular summary of the regression equations along with their supporting LRI scores is provided in Table 3. LRI averages and IRI results from each test are also provided. A plot of Table 3 regression equations is provided in Figure 16.

The LRI_{PS} scores for the 11 bridges are provided in Table 4. The figures were made by plugging each bridge's posted speed into their respective regression equations and then dividing the result by 100,000 (to make the index more manageable). Table 4 results are plotted in Figure 17.

The LRI_{PS} ranking of the 11 bridges from smoothest ride to roughest ride was 08, 11, 02, 01, 10, 09, 05, 04, 07, 06, and 03 with the majority of the tested bridges scoring from uncomfortable to tolerable. The average IRI scores tabulated in Table 3 are repeated in Table 4. The IRI ranking was 08, 07, 09, 03, 06, 10, 02, 11, 04, 01, and 05, which does not correspond with the panel ranking. Testing of the 11 bridges suggested the LRI_{PS} indexing system could be defined as shown in Table 5.

The intention for field implementation of the LRI indexing system is that it will require only a single test to be run at posted speed. To illustrate that implementation testing does not require a multi-speed regression analysis, a single-speed retest of the Table 2 bridges was conducted approximately one year after the regression-based testing was carried out.

Table 2
Summary of bridges tested

Bridge ID	Name	Bridge Inventory Number & Posted Speed Limit (mph)	Location	Coordinates
01	Cooper Bayou Bridge	8173600651 55 mph	Port Hudson Cemetery Rd (LA 3113)	30°39'16.56"N 91°15'44.42"W
02	Bayou Baton Rouge Bridge	2530201191 55 mph	East Mt Pleasant Rd (LA 64)	30°38'52.08"N 91°13'40.12"W
03	Bayou Baton Rouge Bridge	0190205372 65 mph	Samuels Rd (US 61)	30°35'35.92"N 91°13'10.34"W
04	Baker Canal Bridge	0190204322 55 mph	Scenic Hwy (US 61)	30°34'47.96"N 91°12'43.24"W
05	Cypress Bayou Bridge	2500102901 50 mph	Main St (LA 19)	30°33'53.24"N 91°10'21.32"W
06	South Canal Bridge	2500106182 55 mph	Main St (LA 19)	30°36'42.08"N 91° 9'47.45"W
07	Redwood Creek Bridge	0600207611 55 mph	Plank Rd (LA 67)	30°39'55.73"N 91° 06'0.47"W
08	White Creek Bridge	0600204151 55 mph	Plank Rd (LA 67)	30°37'1.09"N 91° 6'54.72"W
09	Comite River Bridge	2550203101 55 mph	Hooper Rd (LA 408)	30°31'50.59"N 91° 5'45.13"W
10	Blackwater Bayou Bridge	8170505291 50 mph	Blackwater Rd (LA 410)	30°35'59.42"N 91° 4'26.04"W
11	Comite River Bridge	8170802401 45 mph	Joor Rd (LA 946)	30°30'47.45"N 91° 4'29.71"W

The retest scores, provided in Table 6, correlate closely with the regression figures (differences were within the margin of error of the regression analysis). Only in the case of bridge 01 was there enough deterioration to shift its position in the ranking, overtaking bridges 09 and 10, and going from a quality of *uncomfortable* to *tolerable*. Bridge 06 changed in quality as well. But, this was because it was considered a borderline case during the initial testing. Bridge 04 was undergoing rehabilitation and could not be run.

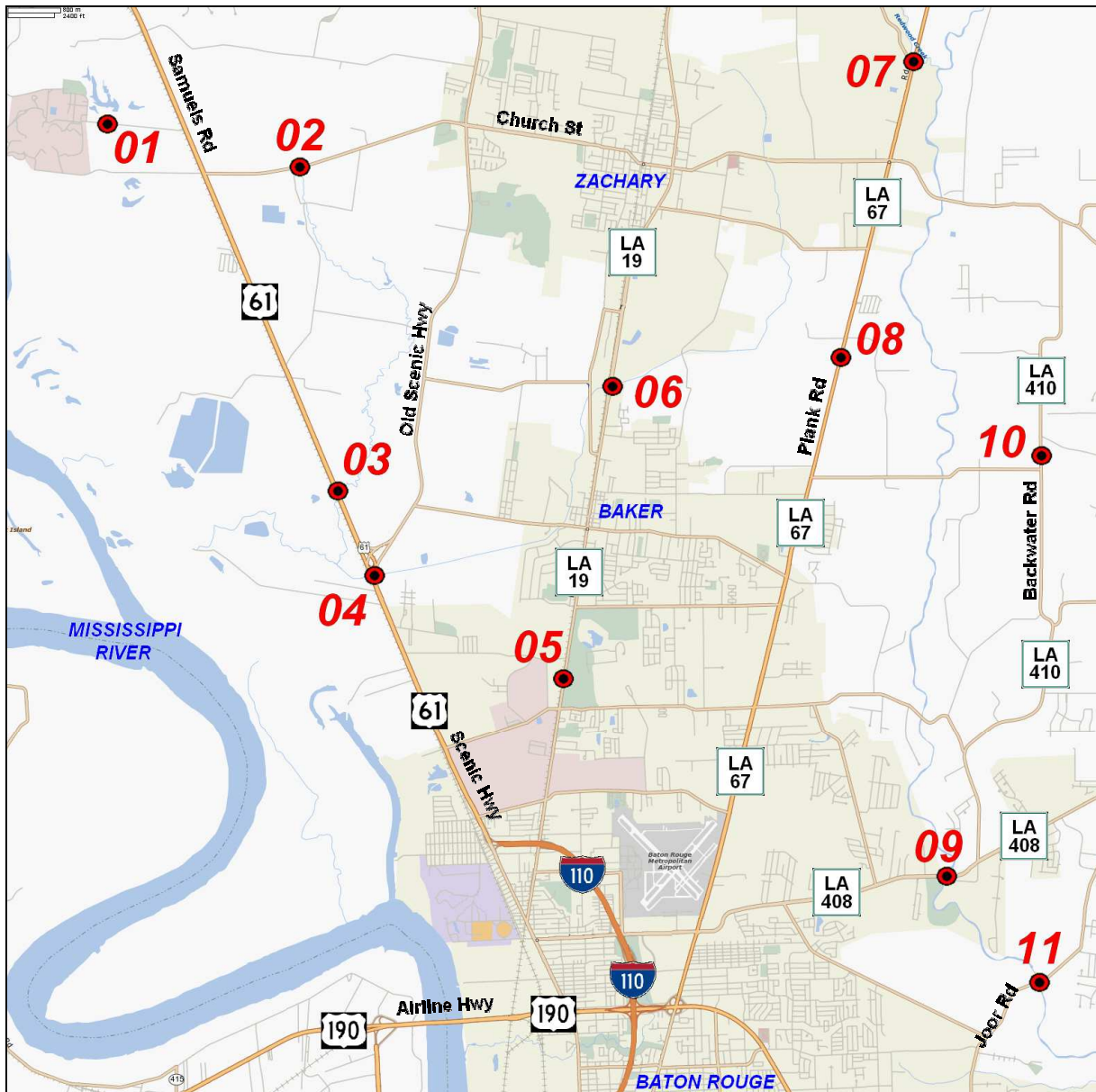


Figure 15
Map of bridges tested

Table 3
Summary of LRI testing

Bridge ID	Profiler Speed (mph)	IRI	Average IRI	LRI Score (ft ⁴ /s ⁸ /100,000)	Exponential Regression of LRI Scores (y: ft ⁴ /s ⁸ /100,000; x: mph)	R² Error
01	30	402	502	0.57523	$y = 0.06997e^{0.0735x}$	0.9655
	30	542		0.58446		
	40	576		1.82943		
	50	563		2.51800		
	60	427		5.51913		
02	30	436	431	0.71178	$y = 0.24601e^{0.0434x}$	0.8098
	30	431		0.84159		
	40	430		2.04221		
	50	430		2.58775		
	60	427		2.60066		
03	30	337	352	1.49445	$y = 0.15997e^{0.088x}$	0.8747
	40	367		8.99070		
	50	357		15.90398		
	60	347		23.22154		
04	30	493	452	0.53569	$y = 0.01719e^{0.1197x}$	0.9166
	40	386		1.84796		
	50	430		13.32764		
	60	499		14.97187		
05	30	484	509	1.66490	$y = 0.21181e^{0.0757x}$	0.9503
	40	519		5.12194		
	50	471		12.83016		
	60	520		17.52771		
	60	550		17.39120		
06	30	339	375	7.35922	$y = 1.86349e^{0.0463x}$	0.8489
	40	373		14.43259		
	50	419		13.25344		
	60	369		35.38341		
07	30	231	268	2.19787	$y = 0.34621e^{0.0670x}$	0.8617
	40	254		5.06408		
	50	295		15.96092		
	60	292		13.98997		
08	30	186	171	0.26329	$y = 0.07058e^{0.0411x}$	0.9675
	40	192		0.31741		
	50	155		0.56855		
	60	152		0.85324		
09	30	302	295	0.70217	$y = 0.13358e^{0.0683x}$	0.8149
	40	287		3.67536		
	50	312		4.06402		
	60	279		6.61355		
10	30	392	378	0.84027	$y = 0.14710e^{0.0667x}$	0.8452
	40	389		3.57373		
	50	352		3.17983		
	60	380		8.08002		
11	30	477	443	0.99448	$y = 0.45197e^{0.0262x}$	0.9962
	40	500		1.30295		
	50	379		1.62450		
	60	416		2.21240		

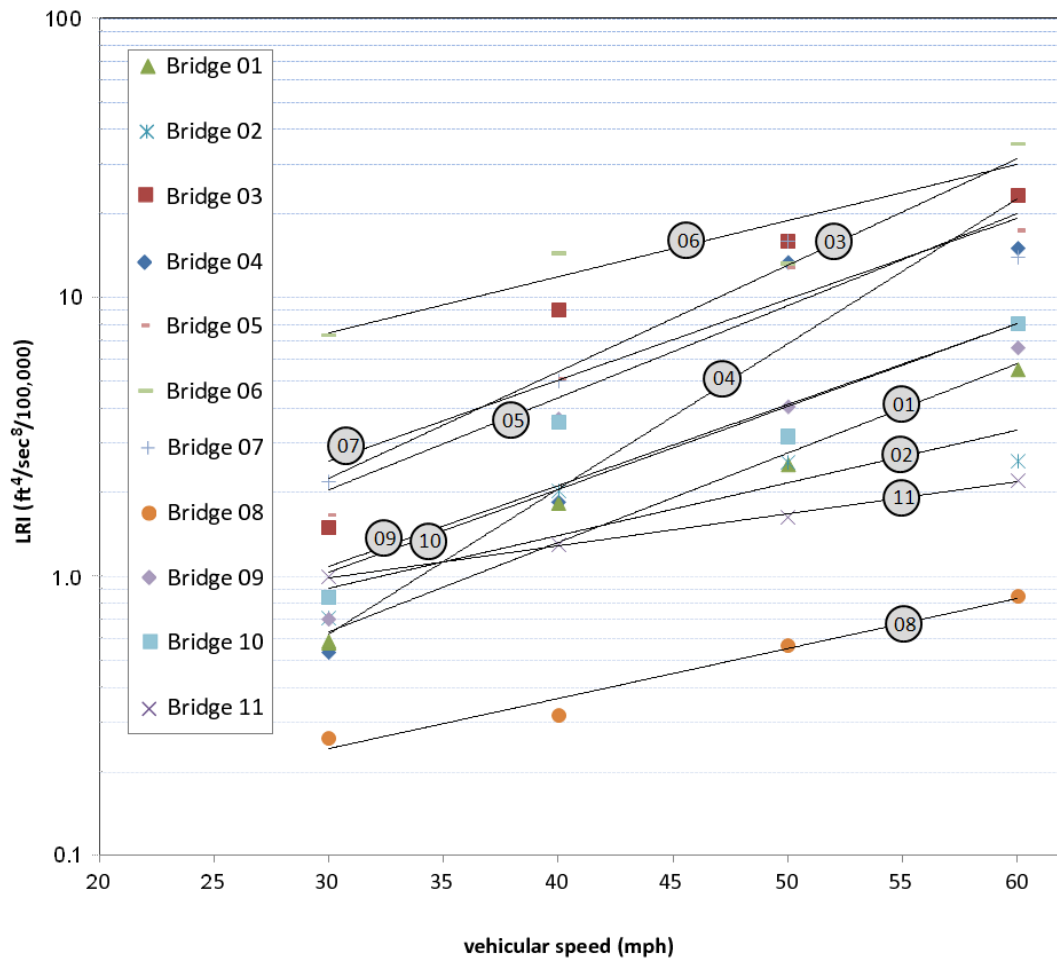


Figure 16
Exponential regression of LRI scores

Table 4
LRI_{PS} scores

Bridge ID	Posted Speed Limit (mph)	LRI_{PS} Scores based on Exponential Regressions (ft⁴/s⁸/100,000)	LRI_{PS} Rating	Average IRI
01	55	4.0	uncomfortable	502
02	55	2.7	uncomfortable	431
03	65	48.8	intolerable	352
04	55	12.4	tolerable	452
05	50	9.3	tolerable	509
06	55	23.8	tolerable	375
07	55	13.8	tolerable	268
08	55	0.7	comfortable	171
09	55	5.7	uncomfortable	295
10	55	4.1	uncomfortable	378
11	45	1.5	uncomfortable	443

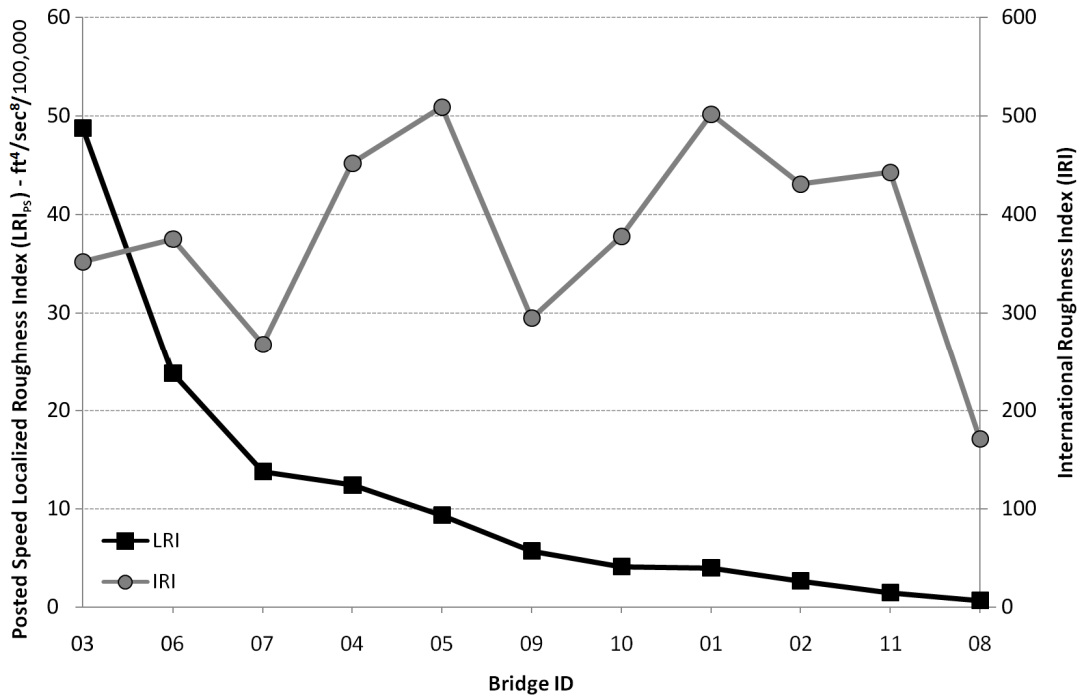


Figure 17
Plot of LRI_{PS} and IRI scores

Table 5
LRI_{PS} indexing system

Condition Rating	Range of LRI_{PS} Scores (ft ⁴ /sec ⁸ /100,000)
unsafe	Greater than 150
intolerable	30.0-150
tolerable	6.00-30.0
uncomfortable	1.20-6.00
comfortable	Less than 1.20

Table 6
Regression-based LRI_{PS} versus single-speed LRI_{PS}

Bridge ID	Posted Speed Limit (mph)	LRI_{PS} Scores based on Exponential Regressions (ft ⁴ /s ⁸ /100,000) ₁	Single-speed LRI_{PS} Scores (ft ⁴ /s ⁸ /100,000) _{2,3}
01	55	4.0 uncomfortable	7.4 <i>tolerable</i>
02	55	2.7 uncomfortable	3.2 uncomfortable
03	65	48.8 intolerable	46.5 intolerable
04	55	12.4 tolerable	<i>Could not run</i>
05	50	9.3 tolerable	12.8 tolerable
06	55	23.8 tolerable	36.3 <i>intolerable</i>
07	55	13.8 tolerable	14.5 tolerable
08	55	0.7 comfortable	0.6 comfortable
09	55	5.7 uncomfortable	3.7 uncomfortable
10	55	4.1 uncomfortable	3.2 uncomfortable
11	45	1.5 uncomfortable	2.6 uncomfortable

1. Ranking: 03, 06, 07, 04, 05, 09, 10, 01, 02, 11, 08

2. Ranking: 03, 06, 07, 04, 05, 01, 09, 10, 02, 11, 08

3. Single-speed testing was conducted approximately one year after the regression-based testing

CONCLUSIONS

It has been recognized that there are inherent limitations associated with the pavement roughness index systems currently in use, like IRI and RN, to locate and quantify certain types of localized pavement distresses found in pavement surface dips and bumps, concrete slab joint faulting, bridge-end bumps, etc. For this reason, a new pavement roughness index for localized pavement distress, herein termed the LRI, was proposed and developed to index such phenomena.

The initial work on developing the LRI was accomplished through the analysis of raw profiler data collected on three different bridges. These bridges were selected to have a wide variety of bridge roughness conditions. This preliminary analysis indicated the squared variance of a high-speed laser profiler's accelerometer output, the LRI, was sufficient to both identify and index bridge-bump type phenomena. Table 1 and Figure 14 summarize the findings. They show that each of the three tested bridges exhibited a unique speed to LRI relationship that could also be used to rate ride quality ranging from comfortable to unsafe.

The LRI_{PS} was developed as a refinement of the preliminary research. This refinement was implemented to ensure that the LRI, which varies with speed, would be able to index ride quality independently of speed. Table 3 summarizes how a LRI_{PS} score is determined. A profiler runs a series of LRI tests at a given site at various speeds. These resulting LRI scores are regressed and regression equations like the ones shown in Table 3 are developed. The LRI_{PS} score for the site is found by plugging the sites posted speed limit into the regression equation. A series of 11 bridges from the northern half of East Baton Rouge Parish were randomly selected to investigate the viability of the LRI_{PS} indexing system. Table 3 summarizes the data collection phase and regression equation development phase of this effort. Table 4 summarizes the resulting LRI_{PS} scores. A summary of the LRI_{PS} indexing system is provided in Table 5.

The intention for field implementation of the LRI indexing system is that it will require only a single test to be run at posted speed. For this reason, a retest of the 11 bridges was undertaken approximately one year after the initial testing. This testing showed that the retest

scores correlated well with the regression based scores (differences were within the margin of error of the regression analysis). A comparison summary of the regression-based and retest scores is provided in Table 6.

The TVTF circuit illustrated in Figure 11 was developed to overcome transportability and suspension degradation issues. It accomplishes this by effectively converting the accelerometer signal of a given profiler into the accelerometer signal of any other profiler. Costs to implement the LRI system is expected to be minimal. A retrofit of a relatively inexpensive accelerometer and/or a Figure 11 prototype circuit board along with associated software is all that should be required to become operational. There will be a need to periodically calibrate the prototype by measuring and inputting vehicular characteristics of the rig being retrofitted (suspension system masses, spring constants, and damping factors). The cost of calibration and the difficulty associated with implementation are also expected to be minimal.

It is also expected that operation of the LRI monitoring system will be very easy requiring little setup or operator attention both prior to and during field testing. Neither is it expected that post-processing will be a problem. Plans are in place to design a stand-alone software program that will accept field collected ASCII files on input and will produce LRI scores on output. Program setup and use are expected to be simple and intuitive.

The value of the LRI system lies in its ability to easily locate and rate localized roughness. This should make it invaluable to maintenance and rehabilitation efforts and for construction QA/QC since there aren't any current, effective means to accomplish this. It is expected that its use in helping field crews to quickly and easily monitor localized distress will generate savings in terms of time, manpower, and money.

Research showed that profile-based indexing systems (like IRI and RN) adequately rate steady-state roughness. But, it was also shown that such systems do have problems rating localized roughness. The LRI_{PS} system, by contrast, has proven itself to be most effective in this area.

RECOMMENDATIONS

It is recommended that the LRI_{PS} indexing system be utilized as a complement to IRI style indexing. Profile-based indexing systems (like IRI and RN) adequately rate steady-state roughness. But, they are known to have problems rating localized phenomena. The LRI_{PS} indexing system was designed to meet this challenge, and its successful performance in field trials underwrites its promotion for use in that area.

Because LRI_{PS} testing was carried out in a limited capacity (a total of only 12 bridges were tested), it is recommended that a more intense program of comprehensive testing be carried out that incorporates more test locations. This is to be done in an effort to verify findings and to refine the system.

The TVTF circuit illustrated in Figure 11 is, theoretically, able to overcome transportability and suspension degradation problems. However, field trials have not yet been undertaken to verify this. It is, therefore, recommended that a program be set up to verify and refine the TVTF design. Also, because the TVTF device is meant to track changing suspension system characteristics of the rig it's associated with, it is also recommended that a methodology be developed that outlines how calibration is to be carried out.

There will be a need to automate all processes associated with LRI_{PS} indexing. At present, indexing is accomplished through a spreadsheet analysis that utilizes macros to arrive at the LRI_{PS} score. It is recommended to develop an automated computer program that is able to identify, isolate, and calculate the LRI_{PS} score for a road anomaly when encountered unexpectedly.

The prototype profiler used in this research had its bridge sensors installed mid-bumper. Although this design was adequate to carry out this pilot research, the fact that the TVTF circuit provided in Figure 11 is designed to simulate a quarter-car indicates that the bridge sensors might, more properly, be installed as closely as possible to the profiler's fender wall. It is, therefore, recommended that future development approach the problem in this manner.

ACRONYMS, ABBREVIATIONS, AND SYMBOLS

ARRB	Australian Road Research Board
EBR	East Baton Rouge
FVTF	Forward Vehicular Transfer Function
ICC	International Cybernetics Corporation
IRI	International Roughness Index
LADOTD	Louisiana Department of Transportation and Development
LQI	Louisiana Quality Initiative
LRI	Localized Roughness Index
LRI _{PS}	Posted Speed Localized Roughness Index
LTRC	Louisiana Transportation Research Center
NCHRP	National Cooperative Highway Research Program
PI	Profile Index
PRC	Project Review Committee
RN	Ride Number
RTRRMS	Response-Type Road Roughness Measuring Systems
RVTF	Reverse Vehicular Transfer Function
TVTF	Translational Vehicular Transfer Function

BIBLIOGRAPHY

1. ASTM (1996). "ASTM E1364: Standard Test Method for Measuring Road Roughness by Static Rod and Level Method." *Annual Book of ASTM Standards*, Vol. 04.03, 750-755.
2. ASTM (1996). "ASTM E950: Standard Test Method for Measuring Longitudinal Profile of Traveled Surfaces with an Accelerometer Established Inertial Profiling Reference." *Annual Book of ASTM Standards*, Vol. 04.03, 702-706.
3. Balogh, L. and Palkovics, L. (2004). *Identification for Control Design of Vehicle Suspension*, 9th Mini Conference on VSDIA 2004, Org.: BME, Budapest.
4. Budras, J. (2001). *A Synopsis on the Current Equipment Used for Measuring Pavement Smoothness*, Pavement Technology, Federal Highway Administration.
5. Gillespie, T.D., et al. (1980). *Calibration of Response-Type Road Roughness Measuring Systems*. National Cooperative Highway Research Program Report 228.
6. Gillespie, T.D., et al. (1987). *Methodology for Road Roughness Profiling and Rut Depth Measurement*. Federal Highway Administration Report FHWA/RD-87-042.
7. Huft, D.L. (1984). "South Dakota Profilometer." *Transportation Research Record 1000*, 1-7.
8. Janoff, M.S., et al. (1985). *Pavement Roughness and Rideability*, National Cooperative Highway Research Program Report 275.
9. Janoff, M.S. (1988). *Pavement Roughness and Rideability Field Evaluation*, National Cooperative Highway Research Program Report 308.
10. Kamen, W.K. and Heck, B.S. (2000). *Fundamentals of Signals and Systems Using the Web and Matlab, Second Edition*, Prentice Hall, Inc.
11. McGillem, C.D. and Cooper G.R. (1984). *Continuous and Discrete Signal and System Analysis, Second Edition*, CBS College Publishing; Holt, Rinehart and Winston (HRW).
12. Sayers, M.W., et al. (1986). *Guidelines for Conducting and Calibrating Road Roughness Measurements*, World Bank Technical Paper No. 46.
13. Sayers, M.W., et al. (1986). *The International Road Roughness Experiment: Establishing Correlation and a Calibration Standard for Measurements*, World Bank Technical Paper No. 45.

14. Sayers, M.W. (1995). "On the Calculation of International Roughness Index from Longitudinal Road Profile." *Transportation Research Record 1501*, 1-12.
15. Sayers, M.W. and Karamihas, S.M. (1996). *Interpretation of Road Roughness Profile Data*, Federal Highway Administration Report FHWA/RD-96/101.
16. Sayers, M.W. and Karamihas, S.M. (1998). *The Little Book of Profiling*, The Regent of the University of Michigan.
17. Shahin, M.Y. (1994). *Pavement Management for Airports, Roads, and Parking Lots*, Chapman & Hall, New York.
18. Zhang, Z. (2002). *Preservation of Bridge Approach Rideability*, Louisiana Quality Initiative, Louisiana Transportation Research Center/Louisiana Department of Transportation and Development.